ORGANOMETALLICS

Article

pubs.acs.org/Organometallics

Synthesis of Group 14 Dipyridinometalloles with Enhanced Electron-Deficient Properties and Solid-State Phosphorescence

Joji Ohshita,*[,†] Kazuya Murakami,[†] Daiki Tanaka,[†] Yousuke Ooyama,[†] Tomonobu Mizumo,[†] Norifumi Kobayashi,[‡] Hideyuki Higashimura,[‡] Takayuki Nakanishi,[§] and Yasuchika Hasegawa[§]

[†]Department of Applied Chemistry, Graduate School of Engineering, Hiroshima University, Higashi-Hiroshima 739-8527, Japan

[‡]Advanced Materials Research Laboratories, Sumitomo Chemical Co. Ltd., 6 Kitahara, Tsukuba 300-3294, Japan

[§]Division of Materials Chemistry, Graduate School of Engineering, Hokkaido University, Sapporo 060-8628, Japan

Supporting Information

ABSTRACT: Silicon- and germanium-bridged bipyridyls were prepared, and their optical and electrochemical properties were investigated. It was found that they exhibited enhanced electron deficiency and phosphorescence properties in comparison to parent bipyridyl. The single-crystal structure of a dipyridinosilole and results of DFT calculations on models are also described.

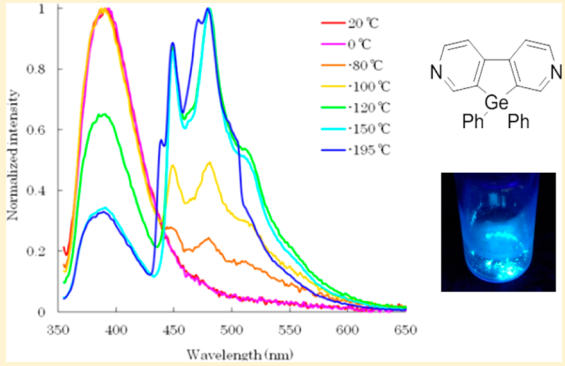

INTRODUCTION

Silole (silacyclopentadiene) derivatives have received a great deal of attention, because of their interesting electronic states and functionalities.[1] In the silole system, an in-phase interaction between silicon σ^* and butadiene π^* orbitals ($\sigma^*-\pi^*$ interaction) lowers the LUMO energy level, giving rise to high electron affinity and enhanced conjugation of the compounds.[2] In 1998, we reported the synthesis of dithienosiloles (DTSs) as the first examples of siloles condensed with heteroaromatic systems, which also possessed low-lying LUMOs.[3] Recently, we prepared also dithienogermoles (DTGs) as the germanium analogues of DTS.[4] Currently, DTS and DTG are widely used as the building units of functional π-conjugated polymers and oligomers, which are applicable to active materials of organic devices, including organic transistors[5] and photovoltaic cells,[4,6] and highly emissive materials.[7] However, to date much less attention has been focused on group 14 metalloles condensed with other heteroaromatic systems, except for some pyrrole- and indole-condensed siloles.[8] Bipyridyl is known as a phosphorescent and highly electron deficient material, and therefore bipyridyls condensed with a group 14 metallole system promise to be exciting compounds. In this paper, we report the synthesis of dipyridinosilole and dipyridinogermole (DPyS and DPyG) for the first time, which exhibit enhanced electron affinity and interesting solid-state phosphorescence.

RESULTS AND DISCUSSION

Three dipyridinometalloles (DPyS1, DPyS2, and DPyG1) were prepared as shown in Scheme 1.[9] The reaction of 3,3′-dilithio-4,4′-bipyridyl with dichlorodiphenylsilane gave 1,1-diphenyldipyridinosilole (DPyS1) in 11% yield, together with many unidentified products, including nonvolatile substances. Bis(methoxyphenyl)dipyridinosilole (DPyS2) was also prepared in a similar fashion in 10% yield. In contrast to the synthesis of DPyS, a similar reaction with dichlorodiphenylgermane proceeded smoothly to provide 1,1-diphenyldipyridinogermole (DPyG1) in 71% yield. Using difluorodiphenylsilane instead of dichlorodiphenylsilane afforded DPyS1 in slightly higher yield

Scheme 1. Synthesis of Group 14 Dipyridinometalloles[a]

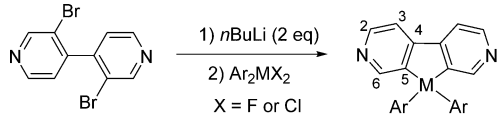

DPyS1 M = Si, Ar = Ph
DPyS2 M = Si, Ar = *p*-MeO(C_6H_4)-
DPyG1 M = Ge, Ar = Ph

[a] Numbering is used for NMR assignments (see Experimental Section)

Received: October 18, 2013

   dx.doi.org/10.1021/om401019b | *Organometallics* XXXX, XXX, XXX−XXX

(13%). These dipyridinometalloles are light brown solids, and repetitive visual observations indicated that they melted without decomposition. The thermal stability of DPyG1 was also confirmed by repetitive DSC analysis (see Figure S-7 in the Supporting Information). The crystal structure of compound DPyS2 was determined by an X-ray diffraction study, and the molecular structure and packing are depicted in Figure 1. The

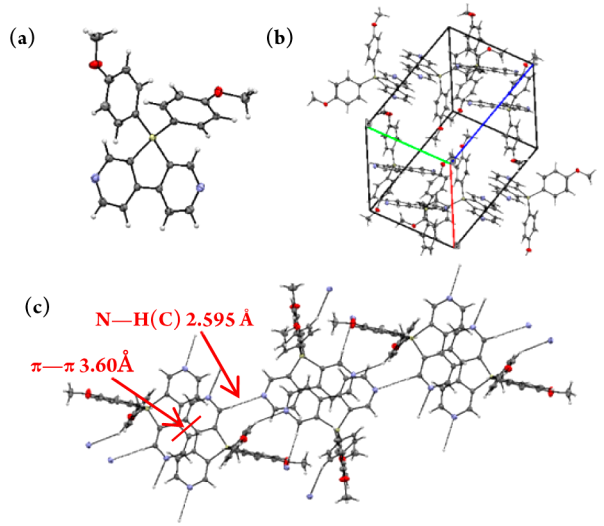

Figure 1. Molecular (a), packing (b), and chain (c) structures of DPyS2 with thermal ellipsoids at the 50% probability level.

tricyclic core of DPyS2 is highly planar (vide infra), and the bond distances and angles of the silole ring system closely resemble those reported for 1,1-dimethyldibenzosilole (DBS),[10] but DPyS2 shows an endocyclic C−Si−C angle (90.69(6)°) slightly smaller than those of DBS (91.05(14) and 91.21(14)°), likely due to the effects of sterically large methoxyphenyl substituents and/or the packing situation. Other silole endocyclic bond angles are 109.55(9) and 109.77(9)° for Si−C═C and 115.07(11) and 114.83(12)°, respectively. The sum of the endocyclic angles is 539.91°, and the silole C═C−C═C dihedral angle is only 0.45°, indicative of high planarity of the silole ring. The crystal packing exhibits an intermolecular face to face interaction between the pyridine rings with the shortest contact of 3.608 Å. In addition, an intermolecular pyridine CH- - -N interaction of 2.595 Å is also observed, thus forming DPyS chains, as shown in Figure 1c.

Absorption maxima of the present dipyridinometalloles were observed at approximately 270 nm (Table 1 and Figure 2), red-shifted from that of 4,4′-bipyridyl (BPy; λ_{max} 237, 270 (shoulder) nm) but slightly blue-shifted from phenyldipyridinophosphole oxide (DPyPO, λ_{max} 276 nm) reported by Durben and Baumgartner (Chart 1).[9] The absorption maxima

Table 1. Optical and Electrochemical Properties of Dipyridinometalloles

compd	UV abs λ_{max}/nm[a]	PL λ_{em}/nm[a,b]	E_{pc}/V[c]
DPyS1	273	420	−1.98
DPyS2	273	408	−2.06
DPyG1	269	400	−1.94

[a]In chloroform at room temperature. [b]Emission maximum excited at the absorption maximum. Absolute PL quantum yields were determined to be less than 2%, by using an integral sphere. [c]Peak potential from Fc/Fc^+ (2 mM in acetonitrile with 0.1 M TBAP at 50 mV/s) .

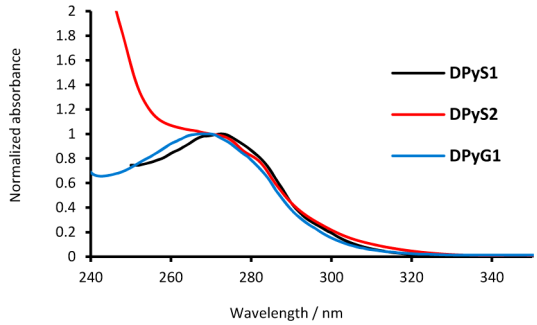

Figure 2. UV spectra of dipyridinometalloles in chloroform.

Chart 1. 4,4′-Bipyridyl and Phenyldipyridinophosphole Oxide

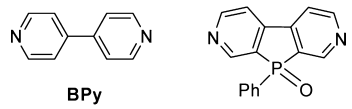

of DPyS1 and DPyS2 were at lower energies in comparison to that of DPyG1. The effects of bridging units pronouncing the conjugation of bipyridyl derivatives thus seem to be enhanced in the order diphenylgermane < diarylsilane < phenylphosphorus oxide. Table 2 represents the results of quantum chemical calculations at the B3LYP/6-31G(d,p) level of theory on nonsubstituted model compounds (DPyS3 and DPyG3 in Figure 3). For comparison, we also examined BPy molecules in either a fully optimized or planarly fixed structure, and the results are also summarized in Table 2. All the computed molecules possess an n-type HOMO and a π-type LUMO, and the TD-DFT calculations indicated that the absorption maxima are assignable to π-type transitions from the HOMO-1 or HOMO-2 to the LUMO. Planar BPy exhibited a $\pi-\pi^*$ band gap smaller than that of the optimized species with a twisted structure, while introduction of a silicon or germanium bridge resulted in an even smaller band gap. Destabilization of the highest occupied π orbital (HOMO-1 or HOMO-2) by introduction of a bridge is likely due to inductive electron donation from the silicon and germanium atoms. For the LUMO, an in-phase $\sigma^*-\pi^*$ interaction is clearly seen to stabilize it, as observed for DTS, DTG, and other silole derivatives (Figure 2 for DPyS3).[2−4] DPyG3 has a $\pi-\pi^*$ band gap slightly larger than that of DPyS3, in accordance with the optical data (Table 2). Cyclic voltammograms of the dipyridinometalloles were examined in acetonitrile containing TBAP (tetrabutylammonium perchlorate) as a supporting electrolyte. As shown in Figure 4, DPyG1 revealed pseudo-reversible reduction properties with a suppressed oxidation counterpart by approximately 70% in the peak height. For DPyS1 and DPyS2, rather weak reduction peaks appeared. The reduction peaks of the metalloles were at potentials higher than that of BPy (E_{pc} = −2.09 V vs Fc/Fc^+), in accordance with the DFT calculations (Table 1), although the differences were only 0.03−0.15 V. They were at potentials lower than that of DPyPO by approximately 0.1−0.2 V.[9]

These dipyridinometalloles were nearly nonemissive in solution at room temperature with quantum efficiencies lower

dx.doi.org/10.1021/om401019b | Organometallics XXXX, XXX, XXX−XXX

Table 2. Frontier Orbital Energies and Characteristics of BPy, DPyS3, and DPyG3, Derived from Calculations at B3LYP/6-31G(d,p)

compd	HOMO-2/eV	HOMO-1/eV	HOMO/eV	LUMO/eV	$\pi-\pi^*$/eV[a]	S0 → T1/eV	interplane angle/deg
BPy[b]	−7.28 (π)	−7.12 (n)	−7.08 (n)	−1.66 (π^*)	5.61	3.46	36.3
BPy (planar)[c]	−7.16 (π)	−7.15 (n)	−7.14 (n)	−1.88 (π^*)	5.28	nd[d]	0
DPyS3[b]	−7.16 (n)	−7.14 (π)	−7.04 (n)	−1.95 (π^*)	5.18	3.16	0
DPyG3[b]	−7.16 (n)	−7.16 (π)	−7.03 (n)	−1.92 (π^*)	5.24	3.20	0

[a]LUMO − (HOMO(π)). [b]Fully optimized. [c]The dihedral angle of C═C−C═C was fixed to 0° and other structural parameters were optimized. [d]Not determined.

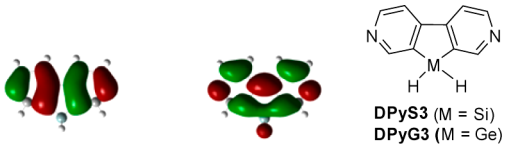

Figure 3. HOMO-1 (left) and LUMO (right) profiles of DPyS3, derived from DFT calculations at the B3LYP/6-31G(d,p) level of theory.

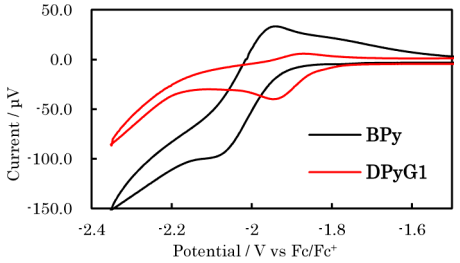

Figure 4. CV profiles of BPy and DPyG1 in acetonitrile.

than 2% (emission maxima are in Table 1). However, they exhibited aggregation-induced emission and showed fluorescence in the solid state at room temperature (lifetime for DPyS1 2.27 ns). Figure 5 depicts temperature-dependent

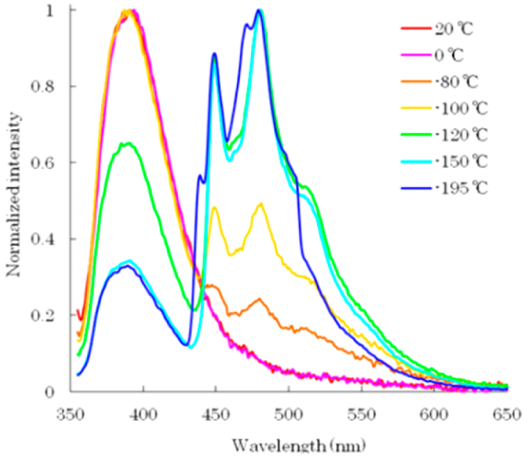

Figure 5. Temperature-dependent emission spectra of DPyG1 in the solid state.

emissive properties of DPyG1 as an example. Interestingly, below −80 °C, new low-energy bands most likely due to phosphorescence appeared and were intensified by lowering the temperature. The phosphorescence of DPyG1 in the solid state at 77 K is composed of multiexponential decays, and the lifetime in longer components is estimated to be approximately 6 μs (Figure 6). The absolute quantum efficiencies were

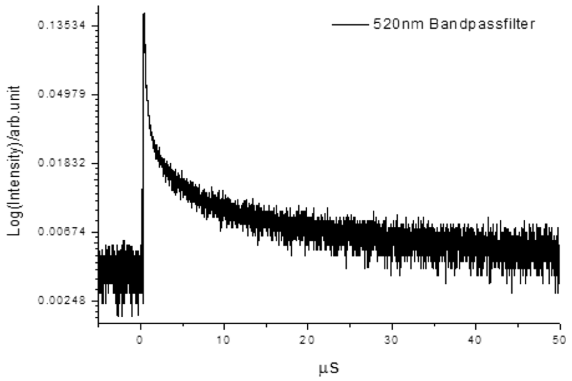

Figure 6. Decay plots of DPyG1 in the solid state at 77 K.

determined in an integration sphere to be 7% for fluorescence and 22% for phosphorescence at 77 K. Phosphorescence radiative and nonradiative decay rate constants were 3×10^4 and 1×10^5 s^{-1}, respectively. DPyS1 and DPyS2 exhibited similar low-temperature phosphorescence, in contrast to BPy, which showed phosphorescence only in solution. The S0 → T1 transition energies obtained by the DFT calculations decrease in the order BPy > DPyG3 > DPyS3 (Table 2). The quantum yields of DPyS1 as solids were found to be less than 1% for both the fluorescence and phosphorescence, while those of DPyS2 could not be determined because of the low intensities. The phosphorescence lifetimes for DPyS1 and DPyS2 were 1.4 and 1.1 μs, respectively. Some dibenzosiloles were recently reported to be phosphorescent at low temperature in glassy solution with the emission quantum efficiencies ranging from 4 to 11%. However, no solid-state phosphorescence was studied.[11]

It may be likely that the $\pi-\pi$ interaction in the solid state affects the optical properties of dipyridinometalloles. To understand this, we carried out DFT calculations of DPyS2 on a single molecule and a $\pi-\pi$ dimeric form based on the crystal structure derived from the X-ray diffraction study (vide supra), indicating intermolecular interaction between the dipyridinosilole units in the LUMO of dimeric form (Figure S-12, Supporting Information). The LUMO is destabilized in the dimer in comparison to the monomer by 0.11 eV. On the other hand, the HOMO is localized on the methoxyphenyl group and is not electronically influenced by the formation of a dimeric form, thus leading to a larger HOMO−LUMO energy gap for the dimer than the monomer by 0.08 eV, in accordance with the fluorescence band of DPyS2 in the solid state being slightly blue shifted from that in chloroform (Figures S-10 and S-11, Supporting Information). However, we could not obtain information about how the $\pi-\pi$ interaction affects the solid-state phosphorescence of DPyS2.

dx.doi.org/10.1021/om401019b | Organometallics XXXX, XXX, XXX−XXX

CONCLUSIONS

In summary, we prepared group 14 dipyridinometalloles and investigated their electrochemical and optical properties. These compounds exhibit pronounced electron affinity in comparison to the parent bipyridyl. In addition, we observed enhanced solid-state phosphorescence of the present dipyridinometalloles. It is likely that introduction of the silicon or germanium bridge fixing the bipyridyl ring minimizes the molecular vibration, thus suppressing the nonradiative decay. Two aryl groups on the bridge may also enhance the solid-state phosphorescence by sterically preventing the aggregation-induced quenching. However, as presented in Figure 1, DPyS2 exhibits intermolecular $\pi-\pi$ stacking in the solid state, which may influence the optical properties in the solid state. Detailed studies on the optical properties of these dipyridinometalloles and structural optimization to enhance the phosphorescence properties are underway.

EXPERIMENTAL SECTION

General Considerations. All reactions were carried out in dry argon. THF that was used as the reaction solvent was distilled from CaH_2 and stored over activated molecular sieves until use. The starting compound 2,2′-dibromo-4,4′-bipyridyl was prepared as reported in the literature.[9] NMR spectra were recorded on Varian 400-MR and System-500 spectrometers. ESI mass spectra were measured on a Thermo Fisher Scientific LTQ Orbitrap XL spectrometer at N-BARD Hiroshima University, while EI mass spectra were recorded on a Shimadzu QP-2020A spectrometer. Room-temperature UV−vis absorption and PL spectra were measured on Hitachi U-3210 and HORIBA FluoroMax-4 spectrophotometers, respectively. The emission quantum yields excited at 350 nm were estimated using a JASCO F-6300-H spectrometer attached to a JASCO ILF-533 integrating sphere unit (φ = 100 mm). The wavelength dependences of the detector response and the beam intensity of the Xe light source for each spectrum were calibrated using a standard light source. Measurements at low temperature (77−300 K) were performed with a nitrogen bath cryostat (Oxford Instruments, Optistat DN) and a temperature controller (Oxford Instruments, ITC 502S), or with a CoolSpeK UV temperature controller (Unisok Co. Ltd., USP-203-A). The quantum yield at 77 K was estimated using the temperature dependence of emission and excitation spectra, following the equation Φ(phosphorescence at 77 K) = Φ(all at 77 K) − Φ(fluorescence at 300 K), assuming that the temperature dependence of the fluorescence intensity is negligible.

Synthesis of Dipyridinometalloles. To a solution of 0.314 g (1.00 mmol) of 2,2′-dibromo-4,4′-bipyridyl in 45 mL of THF was added dropwise 1.22 mL (2.00 equiv) of a 1.64 M *n*-butyllithium solution in hexane at −85 °C, and the mixture was stirred at this temperature for 1 h. To this was added 0.21 mL (1.0 equiv) of dichlorodiphenylsilane, and the resulting mixture was immediately heated to reflux and stirred for 15 min. The mixture was cooled to room temperature and was poured into water. The organic layer was separated, and the aqueous layer was extracted with chloroform. The organic layer and the extracts were combined and dried over anhydrous magnesium sulfate. After evaporation, the residue was chromatographed on silica gel with hexane/ethyl acetate 1/1 as eluent, followed by recrystallization of the crude solids from hexane/ethyl acetate to afford DPyS1 in 11% yield (0.038 g, 0.011 mmol) as an off-white solid: mp 169.7−172.5 °C; EI-MS *m*/*z* 336 [M^+]; ^{1}H NMR ($CDCl_3$) δ 7.40 (td, 4H, *J* = 6.8, 1.2 Hz, *m*-Ph), 7.48 (tt, 2H, *J* = 6.8, 1.2 Hz, *p*-Ph), 7.65 (dt, 4H, *J* = 6.8, 1.2 Hz, *o*-Ph), 7.80 (dd, 2H, *J* = 5.2, 1.2 Hz, pyridine ring H), 8.80 (d, 2H, *J* = 5.2 Hz, pyridine ring H), 9.03 (br s, 2H, pyridine ring H); ^{13}C NMR ($CDCl_3$) δ 117.01 (C3), 128.49 (*m*-Ph), 129.92 (C5), 130.72 (*i*-Ph), 130.95 (*p*-Ph), 135.41 (*o*-Ph), 152.16 (C2), 153.93 (C4), 154.72 (C6); ESI exact MS calcd for $C_{22}H_{17}N_2Si$ [M + H^+] 337.11555, found 337.11612.

Using Ph_2SiF_2 instead of Ph_2SiCl_2 resulted in a slightly higher yield of DPyS1 (13%). DPyS2 was synthesized in a fashion similar to that above, by using dichlorobis(4-methoxyphenyl)silane instead of dichlorodiphenylsilane, as light brown solids in 10% yield after purification by silica gel chromatography, followed by recycling preparative GPC with toluene as eluent: mp 162.1−163.2 °C; EI-MS *m*/*z* 396 [M^+]; ^{1}H NMR ($CDCl_3$) δ 3.81 (s, 6H, Me), 6.93 (d, 4H, *J* = 8.2 Hz, Ph), 7.55 (d, 4H, *J* = 8.2 Hz, Ph), 7.79 (d, 2H, *J* = 5.2 Hz, pyridine ring H), 8.78 (d, 2H, *J* = 5.2 Hz, pyridine ring H), 8.99 (s, 2H, pyridine ring H); ^{13}C NMR ($CDCl_3$) δ 55.11 (Me), 114.30 (*m*-Ph), 116.94 (C3), 120.69(*i*-Ph), 131.42 (C5), 137.06 (*o*-Ph), 151.98 (C2), 153.75 (C4), 154.67 (C6), 161.85 (*p*-Ph); ESI exact MS calcd for $C_{24}H_{21}O_2N_2Si$ [M + H^+] 397.13668, found 397.13745.

Compound DPyG1 was synthesized in a fashion similar to that above, by using dichlorodiphenylgermane instead of dichlorodiphenylsilane, as off-white solids in 71% yield after purification by silica gel chromatography: mp 173.9−174.9 °C; EI-MS *m*/*z* 382 [M^+]; ^{1}H NMR ($CDCl_3$) δ 7.38−7.47 (m, 6H, *m*- and *p*-Ph), 7.57 (dt, 4H, *J* = 6.4, 1.6 Hz, *o*-Ph), 7.85 (dd, 2H, *J* = 5.2, 0.8 Hz, pyridine ring H), 8.80 (d, 2H, *J* = 5.2 Hz, pyridine ring H), 9.00 (d, 2H, *J* = 0.8 Hz, pyridine ring H); ^{13}C NMR ($CDCl_3$) δ 117.60 (C3), 128.87 (*m*-Ph), 130.31(*p*-Ph), 132.50 (C5 or *i*-Ph), 132.79 (C5 or *i*-Ph), 134.50 (*o*-Ph), 151.58 (C2), 152.49 (C4), 154.34 (C6); ESI exact MS calcd for $C_{22}H_{17}N_2Ge$ [M + H^+] 383.05980, found 383.06036.

ASSOCIATED CONTENT

Supporting Information

A CIF file, text, figures, and tables giving crystallographic data, details of the theoretical calculations, NMR spectra of the presently prepared dipyridinometalloles, a DSC profile of DPyG1, CVs and temperature dependent emission spectra of DPyS1 and DPyS2, and room-temperature emission spectra of DPyS1, DPyS2, and DPyG1 in chloroform. This material is available free of charge via the Internet at http://pubs.acs.org.

AUTHOR INFORMATION

Corresponding Author

*E-mail for J.O.: jo@hiroshima-u.ac.jp.

Notes

The authors declare no competing financial interest.

ACKNOWLEDGMENTS

This work was supported by a Grant-in-Aid for Scientific Research on Innovative Areas “New Polymeric Materials Based on Element-Blocks (No. 2401)” of The Ministry of Education, Culture, Sports, Science, and Technology of Japan.

REFERENCES

(1) Tamao, K.; Uchida, M.; Izumikawa, T.; Furukawa, K.; Yamaguchi, S. *J. Am. Chem. Soc.* **1996**, *116*, 11974.

(2) (a) Yamaguchi, S.; Tamao, K. *Chem. Lett.* **2005**, *34*, 2. (b) Yamaguchi, S.; Tamao, K. *J. Chem. Soc., Dalton Trans.* **1998**, 3693.

(3) (a) Ohshita, J.; Nodono, M.; Watanabe, T.; Ueno, Y.; Kunai, A.; Harima, Y.; Yamashita, K.; Ishikawa, M. *J. Organomet. Chem.* **1998**, *553*, 487. (b) Ohshita, J.; Nodono, M.; Kai, H.; Watanabe, T.; Kunai, A.; Komaguchi, K.; Shiotani, M.; Adachi, A.; Okita, K.; Harima, Y.; Yamashita, K.; Ishikawa, M. *Organometallics* **1999**, *18*, 1453. (c) Ohshita, J.; Kai, H.; Takata, A.; Iida, T.; Kunai, A.; Ohta, N.; Komaguchi, K.; Shiotani, M.; Adachi, A.; Sakamaki, K.; Okita, K. *Organometallics* **2001**, *20*, 4800.

(4) Ohshita, J.; Hwang, Y.-M.; Mizumo, T.; Yoshida, H.; Ooyama, Y.; Harima, Y.; Kunugi, Y. *Organometallics* **2011**, *30*, 3233.

(5) Lu, G.; Usta, H.; Risko, C.; Wang, L.; Facchetti, A.; Ratner, M. A.; Marks, T. J. *J. Am. Chem. Soc.* **2008**, *130*, 7670.

(6) (a) Chen, J.; Cao, Y. *Macromol. Rapid Commun.* **2007**, *28*, 1714. (b) Ohshita, J. *Macromol. Chem. Phys.* **2009**, *210*, 1360. (c) Li, Y.-F.

Acc. Chem. Res. **2012**, *45*, 723. (d) Hou, J.; Chen, H.-Y.; Zhang, S.; Li, G.; Yang, Y. *J. Am. Chem. Soc.* **2008**, *130*, 16144. (d) Chu, T.-Y.; Lu, J.; Beaupre, S.; Zhang, Y.; Pouliot, J.-R.; Wakim, S.; Zhou, J.; Leclerc, M.; Li, Z.; Ding, J.; Tao, Y. *J. Am. Chem. Soc.* **2011**, *133*, 4250. (e) Guo, X.; Zhou, N.; Lou, S. J.; Hennek, J. W.; Ortiz, R. P.; Butler, M. R.; Boudreault, P.-L. T.; Strzalka, J.; Morin, P.-O.; Leclerc, M.; Navarrete, J. T. L.; Ratner, M. A.; Chen, L. X.; Chang, P. H.; Facchetti, A.; Marks, T. J. *J. Am. Chem. Soc.* **2012**, *134*, 18427. (f) Gendron, D.; Morin, P. O.; Berrouard, P.; Allard, N.; Aich, B. R.; Garon, C. N.; Tao, Y.; Leclerc, M. *Macromolecules* **2011**, *44*, 7188. (g) Amb, C. M.; Chen, S.; Graham, K. R.; Subbiah, J.; Small, C. E.; So, F.; Reynolds, J. R. *J. Am. Chem. Soc.* **2011**, *133*, 10062. (h) Small, C. E.; Chen, S.; Subbiah, J.; Amb, C. M.; Tsang, S. W.; Lai, T. H.; Reynolds, J. R.; So, F. *Nat. Photonics* **2012**, *6*, 115. (i) Ohshita, J.; Miyazaki, M.; Zhang, F.−B.; Tanaka, D.; Morihara, Y. *Polym. J.* **2013**, *45*, 979.

(7) (a) Ohshita, J.; Kurushima, Y.; Lee, K.-H.; Ooyama, Y.; Harima, Y. *Organometallics* **2007**, *26*, 6591. (b) Ohshita, J.; Kimura, K.; Lee, K.−-H.; Kunai, A.; Kwak, Y.-W.; Son, E.-C.; Kunugi, Y. *J. Polym. Sci., Part A: Polym. Chem.* **2007**, *45*, 4588. (c) Ohshita, J.; Tominaga, Y.; Mizumo, T.; Kuramochi, Y.; Higashimura, H. *Heteroat. Chem.* **2011**, *22*, 514. (d) Ohshita, J.; Tominaga, Y.; Ooyama, Y.; Mizumo, T.; Kobayashi, N.; Higashimura, H. *Dalton Trans.* **2013**, *39*, 9314.

(8) (a) Ohshita, J.; Lee, K.-H.; Kimura, K.; Kunai, A. *Organometallics* **2004**, *24*, 5622. (b) Shimizu, M.; Mochida, K.; Hiyama, T. *Angew. Chem., Int. Ed.* **2008**, *47*, 9760. (c) Mochida, K.; Shimizu, M.; Hiyama, T. *J. Am. Chem. Soc.* **2009**, *131*, 8350. (d) Shimizu, M.; Mochida, K.; Asai, Y.; Yamatani, A.; Kaki, R.; Hiyama, T.; Nagai, N.; Yamagishi, H.; Furutani, H. *J. Mater. Chem.* **2012**, *22*, 4337.

(9) A similar reaction to produce dipyridinophosphole was recently reported. See: Durben, S.; Baumgartner, T. *Angew. Chem., Int. Ed.* **2011**, *50*, 7948.

(10) Mewes, J.; Lerner, H.-W.; Bolte, M. *Acta Crystallogr., Sect. E* **2009**, DOI: 10.1107/S1600536809003614.

(11) Yabusaki, Y.; Ohshima, N.; Kondo, H.; Kusamoto, T.; Yamanoi, Y.; Nishihara, H. *Chem. Eur. J.* **2010**, *16*, 5581.